Methoxy-Substituted Phenalenyl-Based Neutral Radical Molecular Conductor

Arindam Sarkar, Sushanta K. Pal, Mikhail E. Itkis, Puhong Liao, Fook S. Tham, Bruno Donnadieu, and Robert C. Haddon*

Departments of Chemistry and Chemical & Environmental Engineering, University of California, Riverside, California 92521-0403

Received January 26, 2009. Revised Manuscript Received March 31, 2009

We report the synthesis, crystallization, and solid-state characterization of spiro-bis(3,7-dimethoxy-1,9-dioxophenalenyl) boron neutral radical **17**; the radical is distinguished by its oxygen functionalization and we show that our strategy of oxygen substitution at the active positions of the phenalenyl units reduces the electrochemical disproportionation potential. The crystal structure shows that the radical exists as a π-dimer at room temperature and a one-dimensional (1D) π-chain of alternating superimposed and partially superimposed phenalenyl units at 100 K. Magnetic susceptibility measurements show that in the solid state, the radical remains paramagnetic but there is significant spin−spin interaction between the molecules along the π-chains. Band structure calculations delineate the response of the electronic structure to the structural changes observed in the crystal lattice, although magnetic and conductivity measurements do not show any sign of a phase transition. The room temperature electrical conductivity ($\sigma_{RT} = 3.0 \times 10^{-3}$ S/cm) apparently results from the discontinuous character of the π-chains formed by the alternating superimposed and nonsuperimposed phenalenyl units.

Introduction

Organic molecular crystals of spin-bearing molecules such as neutral π-radicals and charge-transfer salts are interesting materials because of their potentials to act as molecular metals. Most of the organic conductors and superconductors are based on charge-transfer salts, which require electron transfer between two components (donor and acceptor) for conduction.[1−4] The concept of using neutral radicals as the building blocks for molecular conductors provides an alternative approach to the conventional charge-transfer organic conductors and superconductors, in which the unpaired electrons of the neutral radicals serve as charge carriers.[5−13] Phenalenyl (PLY)-based radicals have been proposed as molecular conductors and superconductors due to their low ionic fluctuation or disproportionation energy.[5] Over the years, progress in phenalenyl chemistry[14−18] has led to the isolation of the radical in the crystalline state through the introduction of bulky substituents which prevent intermolecular π- and σ-association.[14,15,17,19−22] However, it has been shown that even the 2,5,8-tri-*tert*-butylphenalenyl radical can undergo intermolecular π-association either by formation of a two-electron bond to form a π-dimer (radical−radical pair) or by formation of a one electron bond to form a π-pimer (radical−cation pair).[18]

* Corresponding author. E-mail: haddon@ucr.edu.

(1) Kepler, R. G.; Bierstedt, P. E.; Merrifield, R. E. *Phys. Rev. Lett.* **1960**, *5*, 503–504.
(2) Bechgaard, K.; Cowan, D. O.; Bloch, A. N. *J. Chem. Soc. Chem. Commun.* **1974**, 937–938.
(3) Haddon, R. C.; et al. *Nature (London)* **1991**, *350*, 320–322.
(4) Hebard, A. F.; Rosseinsky, M. J.; Haddon, R. C.; Murphy, D. W.; Glarum, S. H.; Palstra, T. T. M.; Ramirez, A. P.; Kortan, A. R. *Nature (London)* **1991**, *350*, 600–601.
(5) Haddon, R. C. *Nature (London)* **1975**, *256*, 394–396.
(6) Haddon, R. C. *Aust. J. Chem.* **1975**, *28*, 2343–2351.
(7) Oakley, R. T. *Can. J. Chem.* **1993**, *71*, 1775–1784.
(8) Andrews, M. P.; Cordes, A. W.; Douglass, D. C.; Fleming, R. M.; Glarum, S. H.; Haddon, R. C.; Marsh, P.; Oakley, R. T.; Palstra, T. T. M.; Schneemeyer, L. F.; Trucks, G. W.; Tycko, R.; Waszczak, J. V.; Young, K. M.; Zimmerman, N. M. *J. Am. Chem. Soc.* **1991**, *113*, 3559–3568.
(9) Cordes, A. W.; Haddon, R. C.; Oakley, R. T.; Schneemeyer, L. F.; Waszczak, J. V.; Young, K. M.; Zimmerman, N. M. *J. Am. Chem. Soc.* **1991**, *113*, 582–588.
(10) Leitch, A. A.; Reed, R. W.; Robertson, C. M.; Britten, J. F.; Yu, X.; Secco, R. A.; Oakley, R. T. *J. Am. Chem. Soc.* **2007**, *129*, 7903–7914.
(11) Robertson, C. M.; Leitch, A. A.; Cvrkalj, K.; Reed, R. W.; Myles, D. J. T.; Dube, P. A.; Oakley, R. T. *J. Am. Chem. Soc.* **2008**, *130*, 8414–8425.
(12) Robertson, C. M.; Leitch, A. A.; Cvrkalj, K.; Myles, D. J. T.; Reed, R. W.; Dube, P. A.; Oakley, R. T. *J. Am. Chem. Soc.* **2008**, *130*, 14791–14801.
(13) Hicks, R. G. *Org. Biomol. Chem.* **2007**, *5*, 1321–1338.
(14) Goto, K.; Kubo, T.; Yamamoto, K.; Nakasuji, K.; Sato, K.; Shiomi, D.; Takui, T.; Kubota, M.; Kobayashi, T.; Yakusi, K.; Ouyang, J. *J. Am. Chem. Soc.* **1999**, *121*, 1619–1620.
(15) Morita, Y.; Aoki, T.; Fukui, K.; Nakazawa, S.; Tamaki, K.; Suzuki, S.; Fuyuhiro, A.; Yamamoto, K.; Sato, K.; Shiomi, D.; Naito, A.; Takui, T.; Nakasuji, K. *Angew. Chem., Int. Ed.* **2002**, *41*, 1793–1796.
(16) Fukui, K.; Sato, K.; Shiomi, D.; Takui, T.; Itoh, K.; Gotoh, K.; Kubo, T.; Yamamoto, K.; Nakasuji, K.; Naito, A. *Synth. Met.* **1999**, *103*, 2257–2258.
(17) Koutentis, P. A.; Chen, Y.; Cao, Y.; Best, T. P.; Itkis, M. E.; Beer, L.; Oakley, R. T.; Brock, C. P.; Haddon, R. C. *J. Am. Chem. Soc.* **2001**, *123*, 3864–3871.
(18) Small, D.; Zaitsev, V.; Jung, Y.; Rosokha, S. V.; Head-Gordon, M.; Kochi, J. K. *J. Am. Chem. Soc.* **2004**, *126*, 13850–13858.
(19) Beer, L.; Mandal, S. K.; Reed, R. W.; Oakley, R. T.; Tham, F. S.; Donnadieu, B.; Haddon, R. C. *Cryst. Growth Des.* **2007**, *7*, 802–809.
(20) Beer, L.; Reed, R. W.; Robertson, C. M.; Oakley, R. T.; Tham, F. S.; Haddon, R. C. *Org. Lett.* **2008**, *10*, 3121–3123.
(21) Zheng, S.; Lan, J.; Khan, S. I.; Rubin, Y. *J. Am. Chem. Soc.* **2003**, *125*, 5786–5791.
(22) Zheng, S.; Thompson, J. D.; Tontcheva, A.; Khan, S. I.; Rubin, Y. *Org. Lett.* **2005**, *7*, 1861–1863.

10.1021/cm900242a CCC: $40.75
Published on Web 05/04/2009

Scheme 1

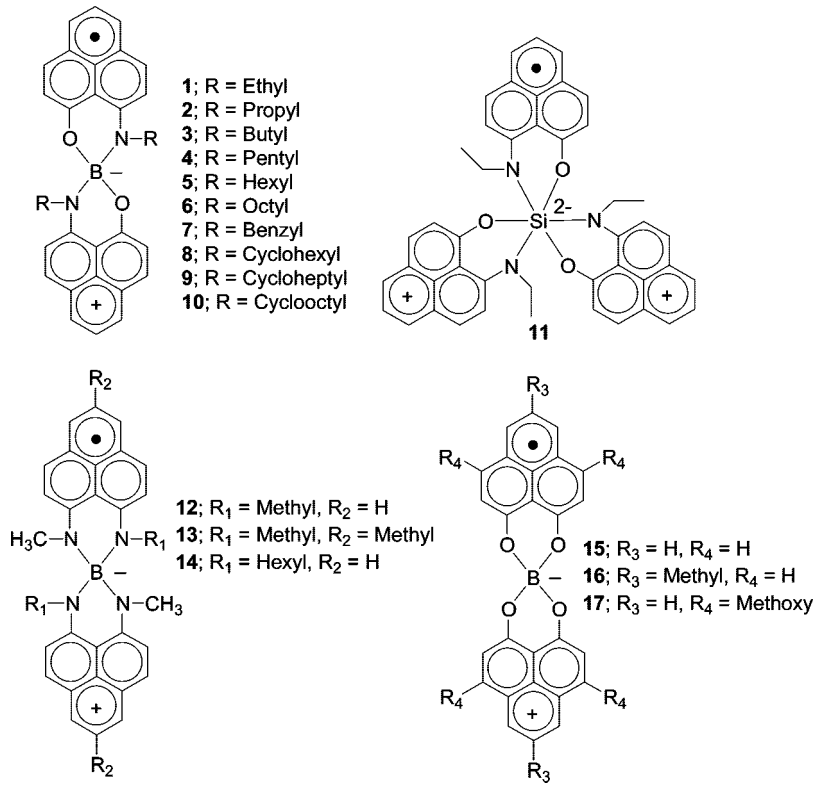

As a part of our efforts to develop phenalenyl-based neutral radical molecular conductors, we have synthesized three families of spiro-bis(1,9-disubstituted-phenalenyl) boron radicals and one tris(1,9-disubstituted phenalenyl) silicon neutral radical (**1**−**16**, Scheme-1). The spiro-conjugation at the boron center leads to an intramolecular $\pi-\pi$ energy level splitting,[23] and the lower level becomes the singly occupied molecular orbital (SOMO). Unlike conventional neutral radicals, the spiro-conjugated radicals give rise to a quarter-filled energy band that significantly reduces the on-site Coulomb correlation energy (U). The other advantage of this class of radicals is that the spiro-geometry severely inhibits the one-dimensional packing that is characteristic of many organic charge transfer salts. Improved conductivities usually result from the design of materials with a higher ratio of W/U, that is, by increasing the bandwidth (W) or by reducing the on-site Coulomb repulsion (U). The on-site Coulomb repulsion energy (U) measures the energy change for an ionic fluctuation and clearly relates to the ease with which a conduction electron can migrate through the lattice. This term is often equated with the electrochemically measurable solution-based disproportionation potential ($\Delta E_{2-1} = E_2^{1/2} - E_1^{1/2}$, eq 1, where $E_1^{1/2}$ and $E_2^{1/2}$ are the first and second reduction potentials of the corresponding cation), and thus U is primarily a molecular property.[24−27] The bandwidth (W) depends on the strength of atomic (or molecular) orbital interactions between neighboring lattice sites and hence is determined by the molecular packing in the solid state, which is difficult to anticipate.

$$\begin{aligned} &R^+ + e^- \rightarrow R^\bullet \quad E_1^{1/2} \\ &R^\bullet + e^- \rightarrow R^- \quad E_2^{1/2} \\ &2R^\bullet \rightarrow R^+ + R^- \quad \Delta E_{2-1} = E_2^{1/2} - E_1^{1/2} \end{aligned} \tag{1}$$

Since the discovery of the first boron-containing neutral radical molecular conductor (**5**),[28] we have reported a variety of packing motifs in the crystal lattices of these radicals, such as π-dimer (**1**,[29,30] **2**,[31] **3**,[29,32] **4**,[33] **6**,[34] **10**,[35] **11**[36]), π-chain (**8**,[37] **9**,[35] **15**,[38] **16**,[38]), π-step (**7**[39]), and monomer (**5**,[28] **12**,[40]

(23) Huang, J.; Kertesz, M. *J. Am. Chem. Soc.* **2003**, *125*, 13334–13335.
(24) Garito, A. F.; Heeger, A. J. *Acc. Chem. Res.* **1974**, *7*, 232–240.
(25) Torrance, J. B. *Acc. Chem. Res.* **1979**, *12*, 79–86.
(26) Boere, R. T.; Moock, K. H. *J. Am. Chem. Soc.* **1995**, *117*, 4755–4760.
(27) Chandrasekhar, V.; Chivers, T.; Parvez, M.; Vargas-Baca, I.; Ziegler, T. *Inorg. Chem.* **1997**, *36*, 4772–4777.
(28) Chi, X.; Itkis, M. E.; Patrick, B. O.; Barclay, T. M.; Reed, R. W.; Oakley, R. T.; Cordes, A. W.; Haddon, R. C. *J. Am. Chem. Soc.* **1999**, *121*, 10395–10402.
(29) Chi, X.; Itkis, M. E.; Kirschbaum, K.; Pinkerton, A. A.; Oakley, R. T.; Cordes, A. W.; Haddon, R. C. *J. Am. Chem. Soc.* **2001**, *123*, 4041–4048.
(30) Itkis, M. E.; Chi, X.; Cordes, A. W.; Haddon, R. C. *Science* **2002**, *296*, 1443–1445.
(31) Chi, X.; Itkis, M. E.; Reed, R. W.; Oakley, R. T.; Cordes, A. W.; Haddon, R. C. *J. Phys. Chem. B* **2002**, *106*, 8278–8287.
(32) Miller, J. S. *Angew. Chem., Int. Ed.* **2003**, *42*, 27–29.
(33) Chi, X.; Itkis, M. E.; Tham, F. S.; Oakley, R. T.; Cordes, A. W.; Haddon, R. C. *Int. J. Quantum Chem.* **2003**, *95*, 853–865.
(34) Liao, P.; Itkis, M. E.; Oakley, R. T.; Tham, F. S.; Haddon, R. C. *J. Am. Chem. Soc.* **2004**, *126*, 14297–14302.
(35) Pal, S. K.; Itkis, M. E.; Tham, F. S.; Reed, R. W.; Oakley, R. T.; Donnadieu, B.; Haddon, R. C. *J. Am. Chem. Soc.* **2007**, *129*, 7163–7174.
(36) Pal, S. K.; Itkis, M. E.; Tham, F. S.; Reed, R. W.; Oakley, R. T.; Haddon, R. *J. Am. Chem. Soc.* **2008**, *130*, 3942–3951.
(37) Pal, S. K.; Itkis, M. E.; Tham, F. S.; Reed, R. W.; Oakley, R. T.; Haddon, R. C. *Science* **2005**, *309*, 281–284.
(38) Mandal, S. K.; Samanta, S.; Itkis, M. E.; Jensen, D. W.; Reed, R. W.; Oakley, R. T.; Tham, F. S.; Donnadieu, B.; Haddon, R. C. *J. Am. Chem. Soc.* **2006**, *128*, 1982–1994.

Scheme 2

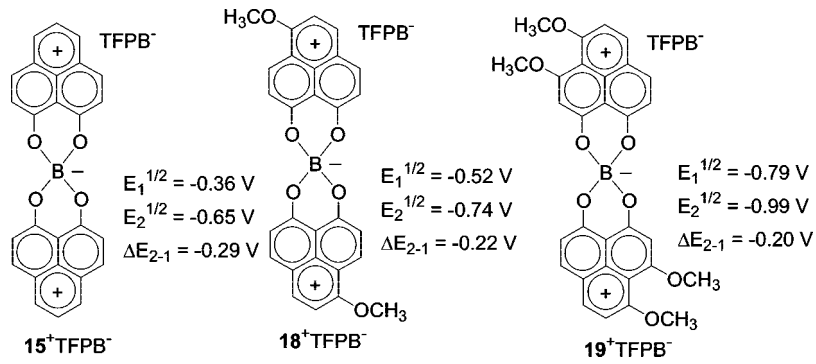

13,[40] **14**,[40]). The radicals **8**, **15**, **16** show the highest conductivities of the neutral radical conductors ($\sigma_{RT} \geq 0.1$ S/cm). Solid-state packing analysis of these three radicals showed that all of them contain a continuous π-chain of superimposed or partially superimposed phenalenyl units, which significantly increases the bandwidth (W).[23,41−44] Moreover, radicals **15** and **16** have the lowest disproportionation energies ($\Delta E_{2-1} \approx -0.30$ V) among this class of molecules and thus these three radicals have the favorable W/U ratio expected for a good neutral radical conductor. The importance of a low disproportionation energy is further emphasized by the relatively low pressed pellet conductivity ($\sigma_{RT} = 2 \times 10^{-3}$ S/cm) of radical **9** which has a π-chain of perfectly superimposed phenalenyl units but a higher value of the disproportionation energy ($\Delta E_{2-1} = -0.44$ V). Thus it is of interest to explore the effect of lowering the disproportionation energy in this system, particularly if the radicals can be induced to crystallize as π-chain radicals.

Although we could lower the ΔE_{2-1} by methoxy substitutions at the spin-bearing carbon, we have been unable to grow single crystals of radicals **18** and **19**; we posit that the difficulties experienced in the crystallization of these new radicals might be due to their low symmetry. Thus we designed a new phenalenone precursor that would preserve the symmetry of the parent spiro-bis(1,9-disubstituted-phenalenyl) boron radical **15**, and in the present manuscript, we report the synthesis, electrochemistry, crystallization, and solid-state properties of a new symmetrically substituted, dimethoxy phenalenyl radical **17** (Scheme 1). As a result of the methoxy substitution at the spin-bearing carbon atoms, the observed disproportionation potential (ΔE_{2-1}) obtained from electrochemistry is significantly lower than those observed for the salts of previously reported spiro-bis(1,9-disubstituted-phenalenyl) boron neutral radicals. The solid-state structure of the radical is unusual in that **17** undergoes a continuous transition from π-dimer at room temperature to a 1D alternating π-chain at low temperatures, without any evidence of a phase transition.

Results and Discussion

We synthesized $\mathbf{18}^+TFPB^-$ and $\mathbf{19}^+TFPB^-$ (Scheme 2), with one and two methoxy groups at spin-bearing carbon atoms of the PLY groups and observed the electrochemistry of these salts. The disproportionation energies of **18** and **19** are $\Delta E_{2-1} = -0.22$ and -0.20 V (Scheme 2), respectively, which is significantly lower than the corresponding unsubstituted compound $\mathbf{15}^+TFPB^-$ ($\Delta E_{2-1} = -0.29$ V).[38,45] Alkoxy substituents in aryl systems are known to act as both π-donors and σ-acceptors[46] and we suggest that the methoxy substituents in **18** and **19** function to lower the ionic fluctuation energy which is implicit in the disproportionation process (eq 1, Scheme 2), as a result of their ability to stabilize the cation via π-donation and the anion via σ-attraction.

Synthesis of 3,7-Dimethoxy-9-hydroxyphenalenone (25). We prepared 3,7-dimethoxy-9-hydroxy phenalenone (**25**) in five steps (Scheme 3), the first of which was the synthesis of 1,3 dimethoxy naphthalene (**21**) from commercially available 1,3 dihydroxy naphthalene (**20**).[47] The acylation step was carried out by following the previously reported procedure for the acylation of 2,7-dimethoxy naphthalene.[48] Polyphosphoric acid was used for the cyclization reaction[49] in order to generate the phenalenone framework (**23**). Demethylation[50] of **23** yielded the hydrogen-bonded trihydroxy species (**24**). Selective remethylation[48] of **24** in the successive step gave the desired ligand (**25**) in an overall yield of about 22%.

Preparation and Electrochemical Properties of Radical 17. The synthesis of radical **17** followed the same basic procedure that has been used to prepare radicals **1**−**16**. We first prepared the chloride salt ($\mathbf{17}^+Cl^-$) and finally employed the tetraphenyl borate anion to obtain the required solubility properties of the salt (Scheme 4). The tetraphenylborate salt ($\mathbf{17}^+BPh_4^-$) was purified as air-stable red crystals by recrystallization from methanol and dichloromethane. The elec-

(39) Pal, S. K.; Itkis, M. E.; Reed, R. W.; Oakley, R. T.; Cordes, A. W.; Tham, F. S.; Siegrist, T.; Haddon, R. C. *J. Am. Chem. Soc.* **2004**, *126*, 1478–1484.
(40) Mandal, S. K.; Itkis, M. E.; Chi, X.; Samanta, S.; Lidsky, D.; Reed, R. W.; Oakley, R. T.; Tham, F. S.; Haddon, R. C. *J. Am. Chem. Soc.* **2005**, *127*, 8185–8196.
(41) Huang, J.; Kertesz, M. *J. Am. Chem. Soc.* **2006**, *128*, 1418–1419.
(42) Bohlin, J.; Hansson, A.; Stafstrom, S. *Phys. Rev. B* **2006**, *74*, 155111.
(43) Huang, J.; Kertesz, M. *J. Am. Chem. Soc.* **2007**, *129*, 1634–1643.
(44) Huang, J.; Kertesz, M. *J. Phys. Chem. A* **2007**, *111*, 6304–6315.
(45) Haddon, R. C.; Chichester, S. V.; Marshall, J. H. *Tetrahedron* **1986**, *42*, 6293–6300.
(46) Swain, C. G.; Unger, S. H.; Rosenquist, N. R.; Swain, M. S. *J. Am. Chem. Soc.* **1983**, *105*, 492–502.
(47) Buu-Hoi, N. P.; Lavit, D. *J. Org. Chem.* **1956**, *21*, 1022–1024.
(48) Haddon, R. C.; Hirani, A. M.; Kroloff, N. J.; Marshall, J. H. *J. Org. Chem.* **1983**, *48*, 2115–2117.
(49) Halton, D. D.; Morrison, G. A. *J. Chem. Res.* **1979**, *1*, 4–5.
(50) Dang, T. D.; Dalton, M. J.; Venkatasubramanian, N.; Johnson, J. A.; Cerbus, C. A.; Feld, W. A. *J. Polym. Sci. Polym. Chem.* **2004**, *42*, 6134–6142.

Scheme 3

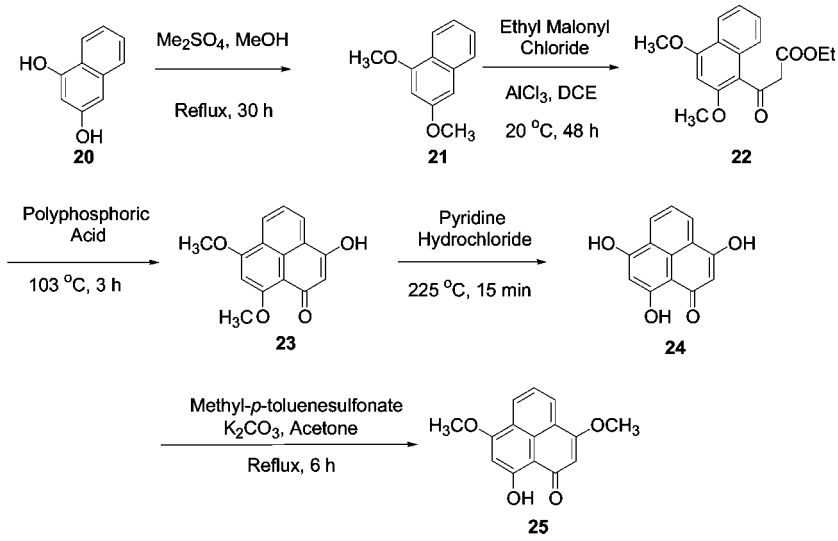

Scheme 4

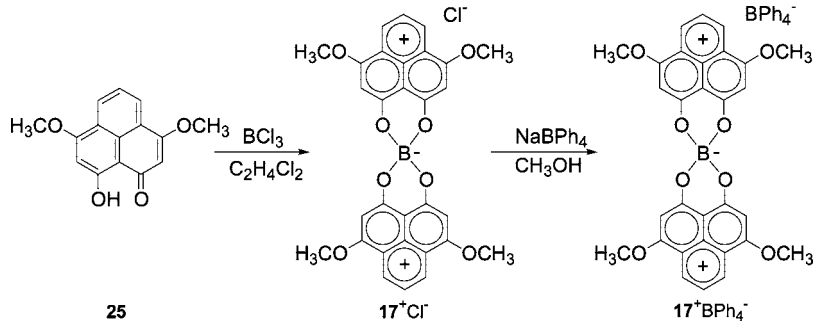

trochemistry of $\mathbf{17}^{+}BPh_4^{-}$ is presented in Figure 1, where it may be seen that the salt shows a well-behaved reversible double reduction corresponding to the successive generation of radical and anion (Scheme 5).

The reduction potentials and the disproportionation energies ($\Delta E_{2-1} = E_2^{1/2} - E_1^{1/2}$) are given in Table 1. The reduction of the new compounds $\mathbf{17}^{+}BPh_4^{-}$, $\mathbf{18}^{+}TFPB^{-}$, and $\mathbf{19}^{+}TFPB^{-}$ might have been expected to occur at less negative potentials than those of ($\mathbf{1}^{+}BPh_4^{-}$) − ($\mathbf{16}^{+}BPh_4^{-}$) based on the electronegativities of the substituents, but are observed to occur at more negative values than those of $\mathbf{15}^{+}BPh_4^{-}$ and $\mathbf{16}^{+}BPh_4^{-}$, apparently as a result of the π-electron donation from the oxygen atoms. However, the disproportionation potential (ΔE_{2-1}) of **17** is lower than those of the previously reported compounds (**1**−**16**) (Figure 2). We attribute the reduced values of ΔE_{2-1} in **17**−**19** to the ability of the methoxy group to function as a π-donor (thereby stabilizing the cation, Scheme 5) and as a σ-acceptor (stabilizing the anion) at the expense of the radical. As discussed above, the ΔE_{2-1} value largely determines the on-site Coulomb correlation energy (U) in the solid state and is well-established as an important discriminator for organic metals.[24,25]

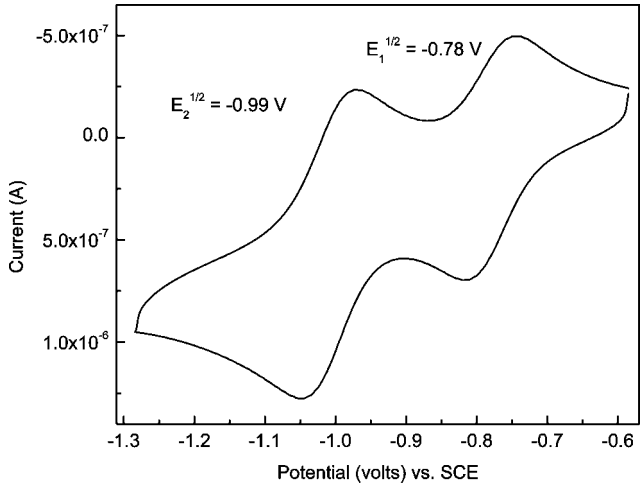

Figure 1. Cyclic voltammetry of $\mathbf{17}^{+}$ BPh_4^{-} in acetonitrile, referenced to SCE via internal ferrocene (not shown).

We crystallized radical **17** by use of a chemical reductant (Scheme 6) in an H-cell and obtained a good yield of high-quality, long red needles of radical crystals. Cobaltocene was used as reductant as its oxidation potential ($E^{1/2} = -0.91$ V) falls slightly below the first reduction potential of $\mathbf{17}^{+}BPh_4^{-}$ salt. To ensure high crystal quality, we loaded the H-cell in a drybox and degassed the solvent (acetonitrile) a minimum of three times on a vacuum line before mixing the reductant and salt. Crystal growth started on the glass frit after 2 h standing, and the crystals reached their optimum size and quality in about 6 h. Though solutions of the radical are extremely oxygen sensitive, the crystals are sufficiently stable to allow ambient chemical analyses, X-ray crystal structures and solid-state measurements.

Scheme 5

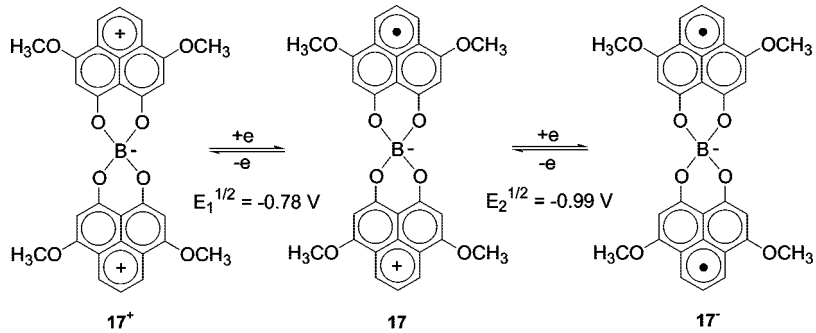

Table 1. Half-Wave Potentials and Disproportionation Potentials (Volts vs SCE) for Phenalenyl-Based Boron and Silicon Salts in CH_3CN[36,38]

salt	structure	$E_1^{1/2}$	$E_2^{1/2}$	ΔE_{1-2}
1$^+BPh_4^-$	[PLY(O,N Et)]$_2$B	−0.75	−1.10	−0.35
2$^+BPh_4^-$	[PLY(O,N Pr)]$_2$B	−0.75	−1.10	−0.35
3$^+BPh_4^-$	[PLY(O,N Bu)]$_2$B	−0.73	−1.09	−0.36
5$^+BPh_4^-$	[PLY(O,N Pt)]$_2$B	−0.74	−1.11	−0.37
6$^+BPh_4^-$	[PLY(O,N Hx)]$_2$B	−0.74	−1.12	−0.38
7$^+BPh_4^-$	[PLY(O,N Bz)]$_2$B	−0.68	−1.02	−0.34
8$^+BPh_4^-$	[PLY(O,N CyHx)]$_2$B	−0.75	−1.12	−0.37
9$^+BPh_4^-$	[PLY(O,N CyHpt)]$_2$B	−0.76	−1.20	−0.44
10$^+BPh_4^-$	[PLY(O,N CyOct)]$_2$B	−0.78	−1.21	−0.43
11$^+BPh_4^-$	[PLY(O,N Et)]$_3$Si	−0.89	−1.24	−0.35
12$^+BPh_4^-$	[PLY(N Me,N Me)]$_2$B	−1.02	−1.37	−0.35
13$^+BPh_4^-$	[5−Me−PLY(NMe,NMe)]$_2$B	−1.06	−1.41	−0.35
14$^+BPh_4^-$	[5 Me−PLY(NMe,NHex)]$_2$B	−1.01	−1.39	−0.38
15$^+TFPB^-$	[PLY(O,O)]$_2$B	−0.36	−0.65	−0.29
16$^+TFPB^-$	[5 Me−PLY(O,O)]$_2$B	−0.36	−0.64	−0.28
17$^+BPh_4^-$	[3,7 OMe−PLY(O,O)]$_2$B	−0.78	−0.99	−0.21
18$^+TFPB^-$	[4 OMe−PLY(O,O)]$_2$B	−0.52	−0.74	−0.22
19$^+TFPB^-$	[3,4 OMe−PLY(O,O)]$_2$B	−0.79	−0.99	−0.20

X-ray Crystal Structure of 17. The structure of **17** was determined at two different temperatures (293 and 100 K) in order to study the interplanar separation as a function of temperature and to test for the presence of phase transitions. Table 2 provides crystal data and Figure 3a shows the ORTEP drawing of radical **17**. The methoxy groups of **17** are found to be coplanar with the rings and thus we conclude that the oxygen atoms are sp^2-hybridized and remain in conjugation with the phenalenyl units in the radical (Figure 3b). The asymmetric unit of the radical is composed of a complete molecule, signifying the nonsymmetric nature of the two halves of the molecule in the solid-state. Although no phase transitions are evident in the measured physical properties, radical **17** undergoes a significant change in its solid-state structure between 293 and 100 K (Table 2 and below), and this transformation exerts a profound effect on the electronic structure. The molecular geometry of **17** differs from that of most of the other radicals of this class because of the considerable bending of one of the phenalenyl units at the two oxygen atoms (O3 and O4, Figure 3b). This kind of bending has been previously observed only in the case of radical **16**, where the ring substituents clearly force the distortion.[38]

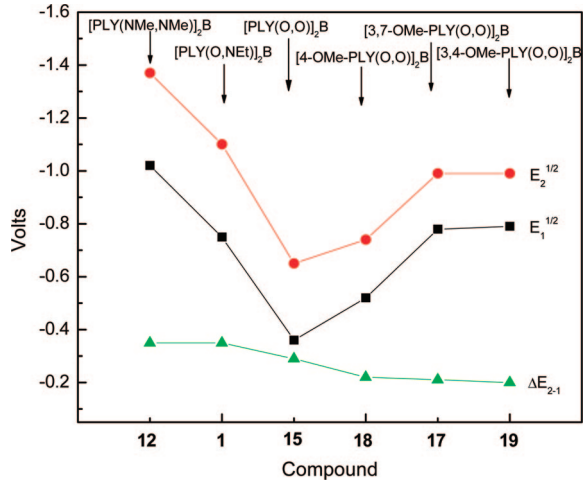

Figure 2. Comparison of $E_1^{1/2}$, $E_2^{1/2}$, and ΔE_{2-1} in different classes of spiro-biphenalenyl boron radicals; **12**(N,N); **1**(N,O); **15**(O,O); **17**, **18**, **19** (methoxy-substituted (O,O)).

Scheme 6

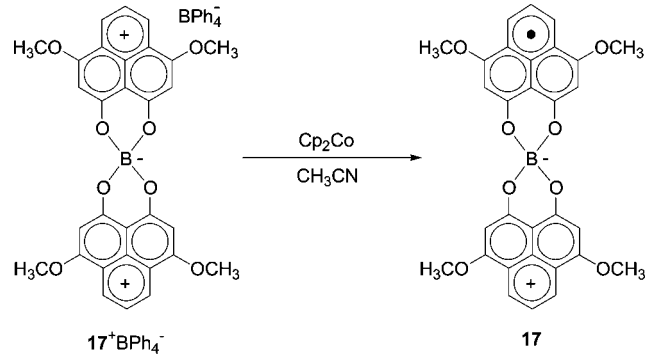

It may be seen from Figure 4 that the solid-state structure of **17** at 293 K consists of π-dimers in which there is almost perfect superposition of the active carbon atoms of one of the phenalenyl units (referred to as PLY-1). The C−C distances between the superimposed phenalenyl rings are within the van der Waals distance for carbon atoms (3.4 Å) but for the nonsuperimposed phenalenyls (referred to as PLY-2), the distances are far from the van der Waals range. The distances between the 6 spin-bearing carbons of superimposed phenalenyl units (PLY-1) at 293 K are 3.31 (2 pairs), 3.32 (2), 3.35 (2), and 3.37 Å (very little spin density), and the interplanar separation is 3.33 Å. It is apparent from the spin-bearing C−C distances that the superimposed phenalenyl units are slightly bowed so that the terminal (3.35 Å) and central (3.37 Å) carbon atoms approach less closely than the carbon pairs (3.31 and 3.32 Å) at the ends of the molecules. Although the interplanar separation between nonsuperimposed phenalenyls is 3.35 Å which is within the

Table 2. Crystal Data for Radical 17 at 100 and 293 K

formula	$C_{30}H_{22}BO_8$	
fw	521.29	
cryst syst	monoclinic	
space group	*P*2(1)/*c*	
Z	4	
T (K)	100(2)	293(2)
a (Å)	17.220 (3)	17.324(6)
b (Å)	10.408 (2)	10.560(3)
c (Å)	13.283 (2)	13.652(5)
α (deg)	90	90
β (deg)	100.181(3)	99.007(7)
γ (deg)	90	90
θ range (deg)	2.30−27.76	2.27−27.10
measured reflections used	5275	5097
final *R* indices[$I > 2\sigma(I)$]	$R_1 = 0.0669$ $wR_2 = 0.1650$	$R_1 = 0.0803$ $wR_2 = 0.1988$
R indices (all data)	$R_1 = 0.0903$ $wR_2 = 0.1770$	$R_1 = 0.1417$ $wR_2 = 0.2372$
mean separation between superimposed phenalenyls (PLY-1)	3.22	3.33
mean separation between partially superimposed phenalenyls (PLY-2)	3.24	3.35
dihedral angles between phenalenyls (deg)	89.8	88.2
bending at O1, O2 (deg)	6.7	6.4
bending at O3, O4 (deg)	22.2	22.7

range of van der Waals distance for carbon atoms, the radical can be recognized as *π*-dimer at 293 K because of its slipped structure and the much longer distances (3.50 and 3.68 Å) between the nearest spin-bearing carbons of this phenalenyl unit (PLY-2), which are clearly out of registry.

The absence of overlap between the spin-bearing carbons of PLY-2 (see band structure calculations) presumably limits the conductivity of the radical at room temperature.

The solid-state structure of radical **17** at 100 K reveals that the radicals pack in two similar kinds of continuous arrays of *π*-stacked neighboring phenalenyl units, denoted by chain-1 and chain-2. The spiro-conjugated one-dimensional chain-1 runs along [2, 2, 0] plane, whereas the spiro-conjugated one-dimensional chain-2 runs along [1, 1, 0] plane (Figure 5). Both chain-1 and chain-2 are orthogonal to each other in the *xy* plane of the unit cell, which corresponds to the face of the platelike crystal. Each chain is arranged in parallel orientation and very short intermolecular carbon−carbon contacts so as to form a polymeric network of neutral radicals. Previously reported radicals **8**, **9**, and **15** were

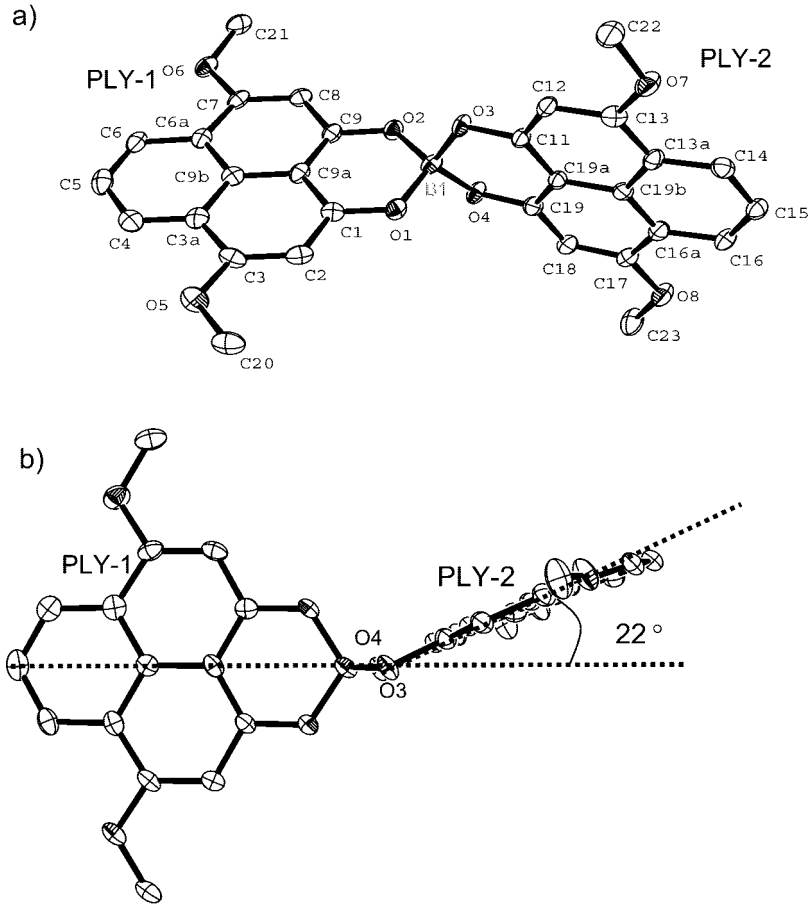

Figure 3. (a) ORTEP diagram of radical **17**. (b) Bending of the phenalenyl unit at the oxygen atoms O3, O4 in **17** at 100 K.

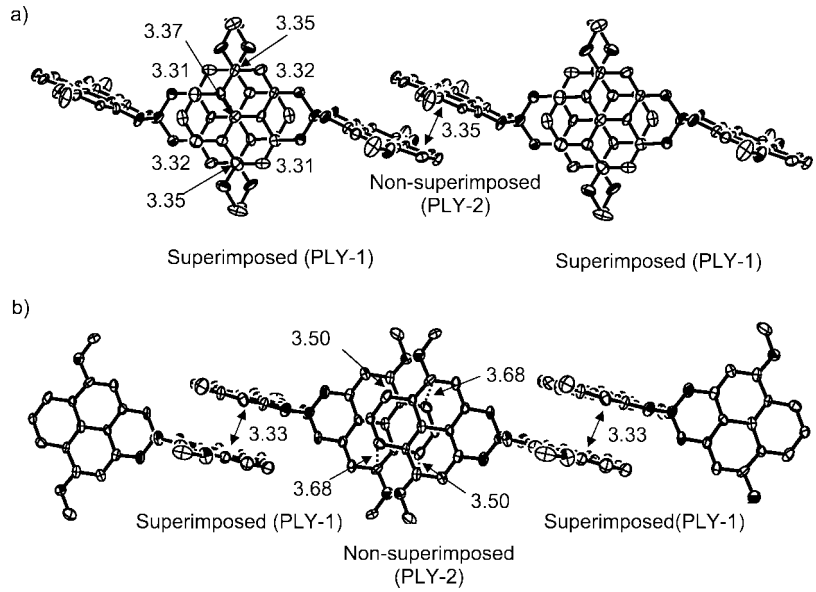

Figure 4. The π-dimer formed by the alternately superimposed and nonsuperimposed phenalenyls at 293 K: (a) superimposed π-overlap, showing the six pairs of spin-bearing carbon atoms of the adjacent phenalenyl units which interact with each other with a closest distance of 3.31 Å, and (b) nonsuperimposed phenalenyls, showing the distances between four pairs of spin-bearing carbon atoms of the adjacent slipped phenaleny rings with a closest distance of 3.50 Å.

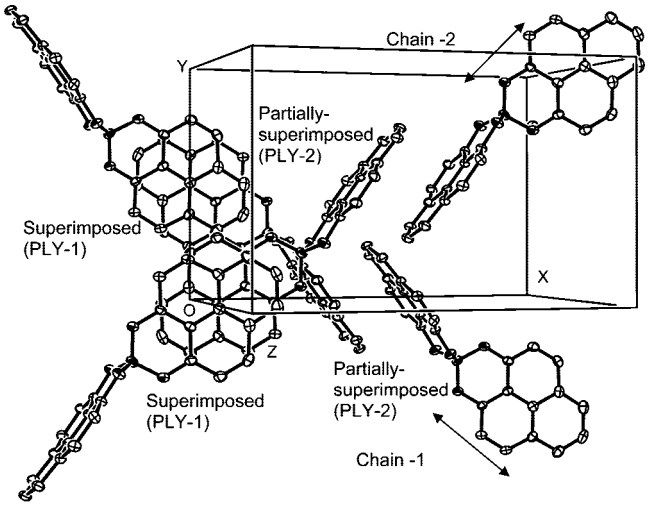

Figure 5. Extended representation of the solid-state packing of **17** at 100 K, showing two similar kinds of infinite spiro-conjugated alternating π-chains (chain-1 and chain-2) of superimposed and partially superimposed phenalenyl units in two different directions (methoxy groups are omitted for clarity).

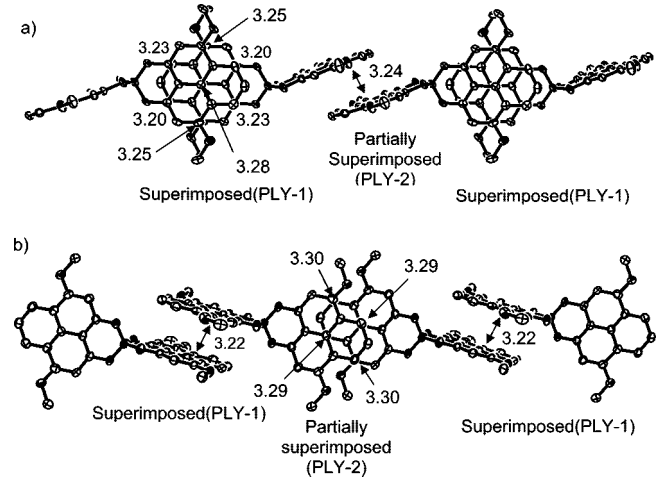

Figure 6. Continuous π-chain formed by the alternate superimposed and partially superimposed π- overlap at 100 K: (a) superimposed π-overlap showing six pairs of spin-bearing carbon atoms of the adjacent phenalenyl units interact with each other with a closest distance of 3.20 Å, and (b) partial π-overlap showing the four pairs of spin-bearing carbon atoms of the adjacent phenalenyl units that interact with each other at a closest distance of 3.29 Å.

involved in similar kinds of continuous π-overlap with adjacent phenalenyl units of nearest neighbors. In the case of radical **17**, one phenalenyl unit (PLY-1) aligns to give a superimposed π-overlap between the neighboring phenalenyl units whereas the other phenalenyl (PLY-2) adopts a slipped π-overlap structure with a bend at the oxygen atoms, as shown in Figure 6. A similar kind of π-chain structure was reported in case of radical **16**, but the main difference is that the bent phenalenyl unit was involved in superimposed π-overlap. In the superimposed π-overlap interaction in **17**, all six of the spin-bearing carbon atoms of the adjacent phenalenyl units are in registry (Figure 6a). The distances between spin-bearing carbons of superimposed phenalenyl units (PLY-1) at 100K are 3.20, 3.23, 3.25, and 3.28 Å. Even at 100 K, the bowed nature of the superimposed phenalenyls has been retained so that the central (3.28 Å) and terminal (3.25 Å) carbon atoms approach less closely than the carbon pairs (3.20 and 3.23 Å) at the ends of the molecules; this leads to a mean plane separation for the superimposed π-structure of 3.22 Å.

In the case of slipped partial π-overlap between phenalenyl units in **17** at 100 K, there is registry between two pairs of fully spin-bearing carbons and between a fully spin-bearing carbon with the central carbon atom (Figure 6b). In fact, the zero value of the spin density found at the central carbon in the simple HMO calculation is accidental; this is an active position, and more sophisticated calculations indicate a finite spin density at the central carbon atom of phenalenyl.[38,51] The distances between spin bearing carbons of partially

(51) McConnell, H. M.; Dearman, H. H. *J. Chem. Phys.* **1958**, *28*, 51–53.

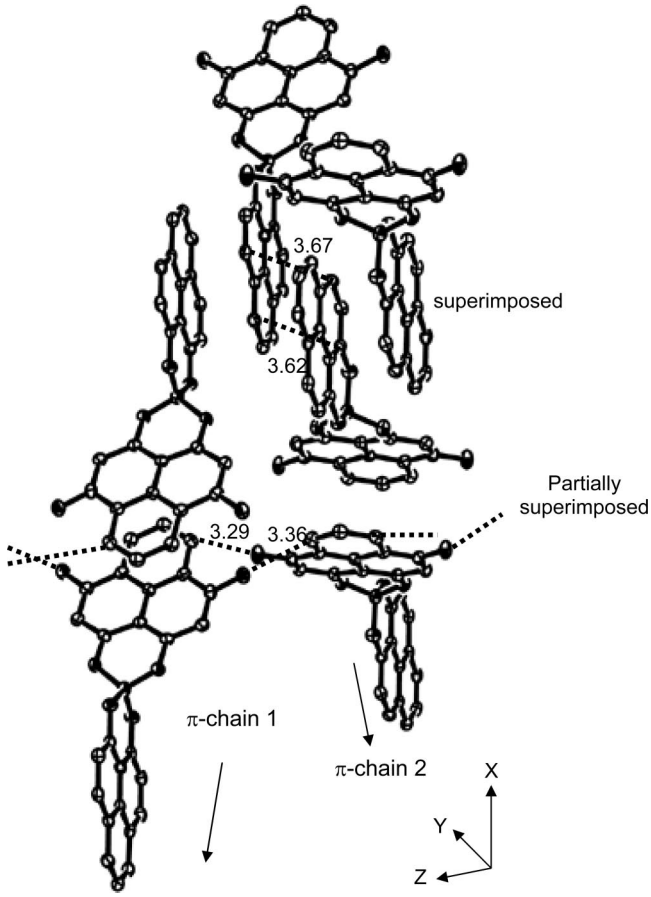

Figure 7. Stacked π chain-1 and π chain-2 interact through a pair of spin bearing carbon atoms (3.62 and 3.67 Å) of superimposed phenalenyl unit in the *y*-direction. The chains also interact through a pair of spin bearing carbon and oxygen atoms of partial superimposed phenalenyl units (3.29 and 3.36 Å) in the *z*-direction at 100 K (OCH_3 groups of superimposed phenalenyls and CH_3 groups of partially superimposed phenalenyls are omitted for clarity).

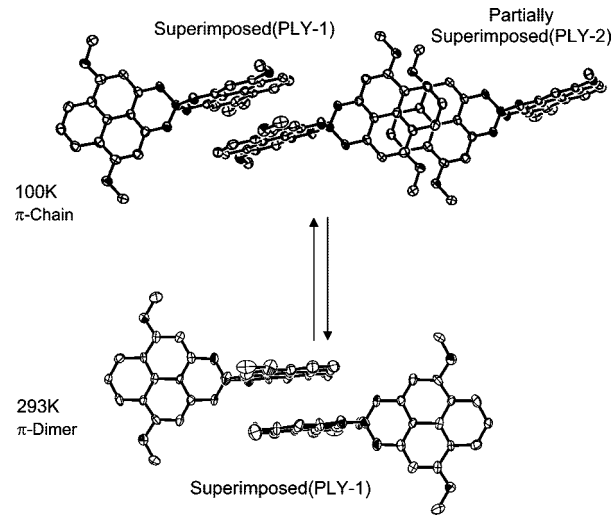

Figure 8. One-dimensional π-chain (100 K) of alternating superimposed and partially superimposed PLY and π-dimer (293 K) structure of radical **17**.

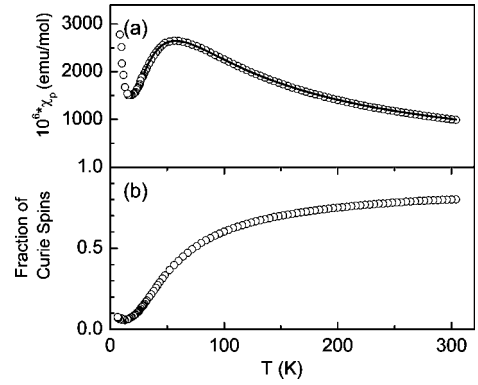

Figure 9. (a) Magnetic susceptibility of crystalline **17** as a function of temperature; the solid line represents the fit to the alternating antiferromagnetic Heisenberg-linear-chain model. (b) Fraction of Curie spins per molecule of crystalline **17** as a function of temperature.

superimposed phenalenyl units (PLY-2) at 100 K are 3.30 and 3.29 Å. The closest C−C distance between phenalenyl units at 100 K are 3.20 Å for superimposed π-overlap and 3.29 Å for partial π-overlap. At low temperature (100 K), the mean plane separations are 3.22 and 3.24 Å for superimposed and partially superimposed phenalenyl units, respectively. These separations may be compared with the mean plane separation (3.21 Å at 130 K, 3.28 Å at 140 K) observed in radical **1** in the vicinity of the phase transition.[52] The compression in the separations between the radical molecules of solid-state **17** at low temperatures is reflected in the higher crystal density and lower unit-cell volume. Figure 7 shows the interactions between chain-1 and chain-2 at 100 K. In the crystal lattice of **17**, the phenalenyl units that take part in the superimposed π-overlap also stack in the direction of the *y*-axis, leading to two weak interchain interactions with closest C−C distances 3.62 and 3.67 Å. On the other hand, the phenalenyl units that take part in the partial π-overlap exhibit a strong and a weak C−O interaction between spin-bearing carbon and oxygen atoms with distances of 3.29 and 3.36 Å, respectively (van der Waals distance between carbon and oxygen atoms is 3.22 Å) along the *z* direction (these distances increase to 3.41 and 3.42 Å at 293 K); further diagrams of the molecular interactions are given in Figures S3−S5 of the Supporting Information.

Thus in the crystal lattice of **17**, at 100K, the molecules form a two-dimensional π-chain structure that is dominated by two diagonal π-chains with very short intermolecular contacts, providing an obvious pathway for conduction, whereas at 293 K, the π-chains have lost their continuity because of the release of π-overlap between the spin-bearing carbons of the partially superimposed phenalenyl units, thereby interrupting the conducting pathway (Figure 8).

Magnetic Susceptibility and Conductivity of 17. Figure 9a shows the magnetic susceptibilities (χ) of **17** over the temperature range 5−305 K. In the high temperature limit ($T > 120$ K), the data can be fit to the Curie−Weiss equation, $\chi = C/(T + \Theta)$ with a Weiss constant of $\Theta = -44$ K, corresponding to an antiferromagnetic interaction between the unpaired spins. The Curie constant of $C = 0.343$ emu K/mol that results from this fitting procedure is ~9% below the value of 0.375 emu K/mol expected for a free-spin neutral radical and is indicative of the inability of the simple Curie−Weiss model to account for the magnetic susceptibility over the full temperature range. In addition, the low-

(52) Haddon, R. C.; Sarkar, A.; Pal, S. K.; Chi, X.; Itkis, M. E.; Tham, F. S. *J. Am. Chem. Soc.* **2008**, *130*, 13683–13690.

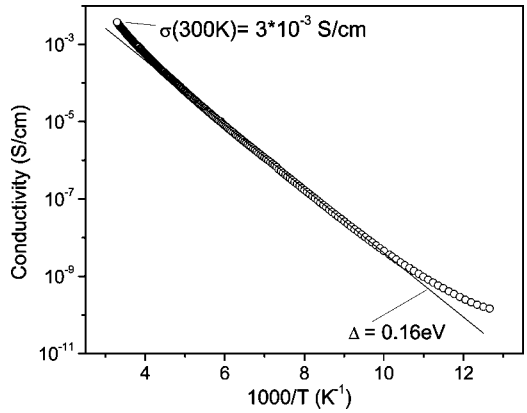

Figure 10. Single-crystal conductivity of **17** as a function of temperature measured along the face (*xy* plane) of the platelike crystal.

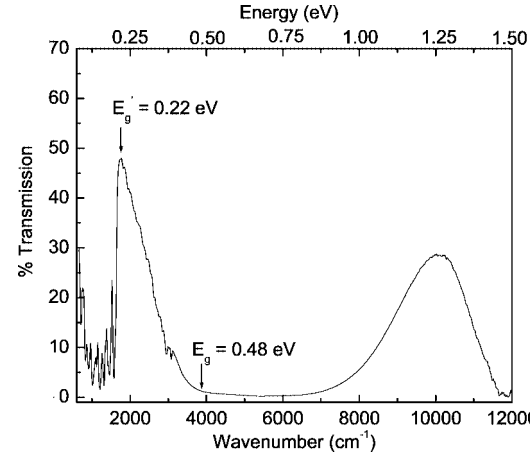

Figure 11. Single-crystal IR and UV−visible transmission spectrum of crystalline **17**.

temperature data show significant deviations from Curie−Weiss behavior because of antiferromagnetic coupling of the unpaired spins, with maxima in the $\chi_p(T)$ curve at $T_{MAX} = 56$ K. To adequately describe the data, we utilized the $S = 1/2$ alternating antiferromagnetic Heisenberg linear chain model[53] in which the antiferromagnetic interaction along the chain alternates between J and αJ values ($0 \leq \alpha \leq 1$) in accord with the solid-state structure (Figure 6); a Curie-type impurity term was introduced to account for the low-temperature paramagnetic tail.[39] This model provides a satisfactory fit to the susceptibility of compound **17** in the temperature range 25−305 K with parameters $J = -35.7$ cm^{-1} and $\alpha = 0.4$, and a concentration of 1.2% of paramagnetic impurities per formula unit. As discussed above, the antiferromagnetic interaction results in a decrease in the effective fraction of Curie spins per molecule (χT/0.375) at lower temperatures (Figure 9b).

The electrical conductivity (σ) of crystalline **17** was measured using four-probe in-line silver paste contacts on the face (*xy* plane of the unit cell) of the platelike crystals and showed semiconducting temperature dependence, activation energy $\Delta = 0.16$ eV, and room temperature conductivity $\sigma_{RT} = 3.0 \times 10^{-3}$ S/cm (Figure 10). A number of crystals were evaluated over the temperature range from 80 to 300 K with identical results.

Electronic Excitations of 17 in the Solid State. To obtain further information on the electronic structure, we measured the absorption spectrum of crystalline **17**. This is possible because of the platelike morphology of the crystals, some of which are quite thin and are suitable for transmission spectroscopy. The results are presented in Figure 11, where we show transmittance (T) measurements made on a single crystal at room temperature. The most important feature in the transmission spectrum is the strong increase of absorption that occurs between 0.22 (E_g') and 0.48 eV (E_g). The bandlike absorption extends through the range 4000−7000 cm^{-1} where the material remains opaque. In the case of an intrinsic semiconductor, the measured optical band gap can be correlated with the activation energy ($\Delta = 0.16$ eV) calculated from the temperature dependence of the conductivity according to $E_g \approx 2\Delta$, although exact identification of the value of optical gap is complicated by broadening of the absorption edge, which is spread between E_g', and E_g. Measurement in the visible region shows that the material is semitransparent in the region 1−2 eV, accounting for the red color of very thin crystals.

Band Electronic Structure of 17. To address the questions of solid-state packing and the electronic structure of **17**, we carried out extended Hückel theory (EHT) band structure calculations[54] on the crystal structures at two different temperatures (293 and 100 K). Such calculations have been very useful in understanding the electronic structure of the organic molecular superconductors[55] and thin-film field effect transistors[56] but it should be noted at the outset that there are certain objections to the application of tight binding band theory to the neutral radical molecular conductors[28] in that the calculations are unable to correctly describe the open-shell electronic structure of the materials as indicated by the occurrence of Curie paramagnetism.

Figure 12 shows the results of the band structure calculations carried out on the lattices found in the X-ray crystal structure of **17** at 293 and 100 K; the eight bands are derived from the SOMO and the LUMO of the four molecules in the unit cell. These basically consist of the symmetric and antisymmetric combinations of the 1,3,7,9-tetrasubstituted phenalenyl cation LUMO.[28,45] Alternatively, they can be viewed as arising from the nonbonding molecular orbitals of each of the phenalenyl units in the unit cell (eight phenalenyl units for **17**). In the band picture, these orbitals (eight for **17**) now accommodate a total of four electrons, leading to a quarter-filled band complex. The most important aspect of the band structure calculations is the extremely narrow bandwidths at room temperature: the valence and conduction band dispersions in the tight binding approximation are less than 0.025 eV along all directions in reciprocal space. This value may be compared with a dispersion of 0.075 eV found in the monomeric hexyl radical (**5**, $\sigma_{RT} = 5 \times 10^{-2}$ S/cm), where all of the interatomic contacts between

(53) Duffy, W.; Barr, K. P. *Phys. Rev.* **1968**, *165*, 647–654.
(54) Hofmann, R. *Solids and Surfaces*; VCH: New York, 1988.
(55) Haddon, R. C.; Ramirez, A. P.; Glarum, S. H. *Adv. Mater.* **1994**, *6*, 316–322.
(56) Haddon, R. C.; Siegrist, T.; Fleming, R. M.; Bridenbaugh, P. M.; Laudise, R. A. *J. Mater. Chem.* **1995**, *5*, 1719–1724.

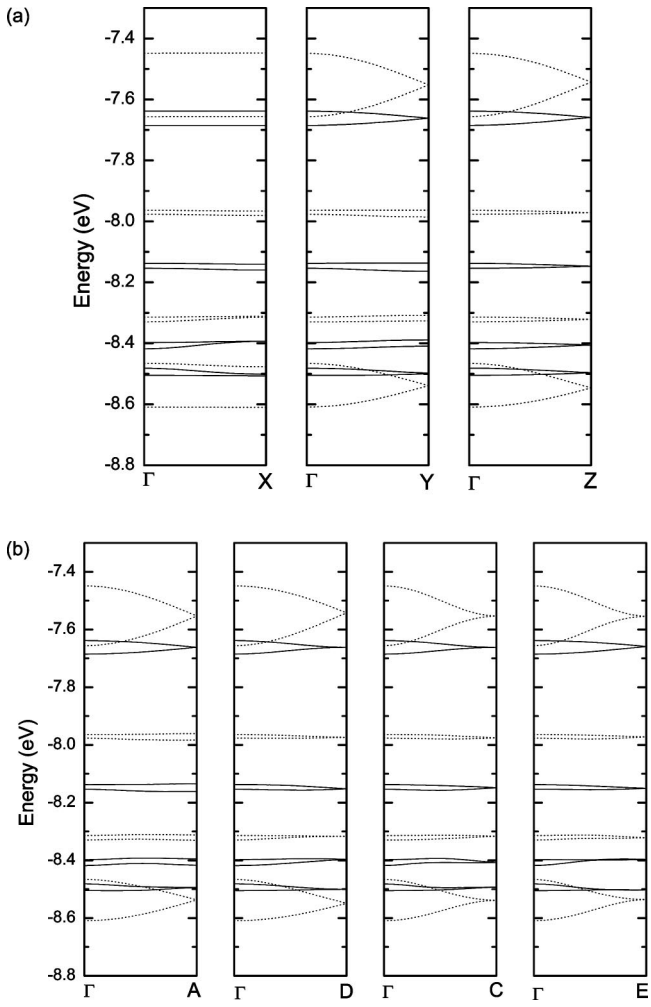

Figure 12. EHT band structure calculated for the experimental structure of crystalline **17**. (a) Dispersions along reciprocal cell axes where $X = [1/2\ 0\ 0]$, $Y = [0\ 1/2\ 0]$, $Z = [0\ 0\ 1/2]$; and (b) dispersions along diagonal directions, where $A = [1/21/2\ 0]$, $D = [1/2\ 0\ 1/2]$, $C = [0\ 1/2\ 1/2]$, and $E = [1/2\ 1/2\ 1/2]$ at 100 K (dotted line) and 293 K (solid line).

molecules are greater than the sum of the carbon···carbon van der Waals separations.[28] Thus it is apparent that the out-of-registry overlap seen in the room temperature structure of **17** effectively drives the bandwidth to zero, and this limits the conductivity (**17**, $\sigma_{RT} = 3 \times 10^{-3}$ S/cm). Because the magnetic interactions are not (solely) dictated by the orbital overlap (Appendix), there is strong antiferromagnetic coupling in **17** that is not present in **5** (which is essentially a Curie paramagnet at temperatures above 10 K).[28]

Conclusion

The first member of a new family of spiro-bis(3,7-dimethoxy 1,9-dioxophenalenyl)boron neutral radical conductors based on the O,O-ligand system has been synthesized and characterized. The strategy of methoxy substitution at the active positions of the PLY system is shown to be successful in lowering the electrochemical disproportionation energy ($\Delta E_{2-1} = E_2^{1/2} - E_1^{1/2}$), of these radicals. However, the room-temperature, solid-state structure of **17** consists of isolated π-dimers, in which the nonsuperimposed phenalenyls are out of registry with respect to the spin density distribution; this severely limits the bandwidth and suppresses the conductivity. The magnetism and the conductivity diverge in this respect: because the magnetic interactions are not (solely) dependent on the orbital overlap (see the Appendix) and there is strong spin−spin coupling in **17**; magnetic susceptibility measurements support the idea that the compound does not exist as an isolated free radical. Thus it is clear that the conductivity of these neutral radicals is strongly influenced by the solid-state packing which ultimately determines the transport properties by modulation of the bandwidth, and it is apparent that there is considerable scope for improving the properties of these compounds. The electrochemical properties of radical **17**, **18**, and **19** show that it is possible to lower the disproportionation energy and thus the solid state U value of these radicals by appropriate substitutions in the PLY nucleus. Because this is a molecular property, the synthesis of such compounds offers an attractive route to the exploration of neutral radical solids of low disproportionation potential.

Experimental Section

General Procedures and Starting Materials. 1,3-Dihydroxynaphthalene (Aldrich), 2,7-dimethoxynaphthalene (Aldrich), boron trichloride (Aldrich), sodium tetraphenylborate (Aldrich), and cobaltocene (Strem) were all commercial products and were used as received. 3,4-Dimethoxy-9-hydroxyphenalenone was prepared according to the literature procedure.[48] 1,2-Dichloroethane was distilled from CaH_2 just prior to use. Toluene was dried over sodium and distilled just prior to use. Acetonitrile was distilled from P_2O_5 and then redistilled from CaH_2 immediately before use. Melting points are uncorrected. The NMR spectra were recorded on a Bruker 300 spectrometer. Infrared spectra were recorded on a Nicolet Nexus 670 FT-IR spectrometer at 2 cm^{-1} resolution. Mass spectra (MALDI) were run on a Voyager-DE STR BioSpectrometry Workstation mass spectrometer. Elemental analyses were performed by the Microanalysis Laboratory, University of Illinois, Urbana, IL.

Preparation of 1,3-Dimethoxynaphthalene (21). 1,3-Dimethoxynaphthalene was prepared according to a modified literature procedure.[47] 1,3-Dihydroxynaphthalene (10 g, 0.062 mol) in 250 mL methanol was treated with dimethylsulfate (14 mL) under argon and the mixture was refluxed for 30 h. The reaction was monitored by thin layer chromatography [$R_f = 0.5$; ethylacetate:petroleum ether, 1:99]. The reaction mixture was allowed to cool to room temperature and the methanol was evaporated under reduced pressure. The residue was dissolved in 200 mL of dichloromethane and washed with 200 mL of ammonia solution and 200 mL of 10% NaOH solution. The solvent was evaporated under reduced pressure and the residue was subjected to column chromatography (SiO_2; ethylacetate:petroleum ether, 1:99) to obtain the title compound as a colorless liquid (11 g, 93%). ^1H NMR ($CDCl_3$): δ 8.20(d, 1H), 7.72(d, 1H), 7.48(t, 1H), 7.37(t, 1H), 6.77(d, 1H), 6.54(d, 1H), 3.99(s, 3H), 3.94(s, 3H).

Preparation of Ethyl-2,4-dimethoxy-1-naphthoylacetate (22). A solution of 1,3-dimethoxynaphthalene (11 g, 0.058 mol) and ethyl malonyl chloride (8.7 mL, 0.07 mol) was stirred in 1,2-dichloroethane under argon. The reaction vessel was immersed in an ice bath and then treated with aluminum chloride (9.3 g, 0.07 mol). The reaction was followed by thin layer chromatography [$R_f = 0.5$; ethylacetate:petroleum ether, 40:60]. After being stirred for 48 h, the reaction mixture was quenched with ice cold 6(N) hydrochloric acid (200 mL). The aqueous fraction was extracted with dichloromethane and the organic fractions combined and dried

over anhydrous sodium sulfate. The solvent was evaporated under reduced pressure and the residue was subjected to column chromatography (SiO_2; ethylacetate:petroleum ether, 10:90) to obtain the title compound as an off-white solid (14.5 g, 87%). Mp 52 °C. MS (ESI), $m/z = 302$. ^{1}H NMR ($CDCl_3$): δ 8.17 (d, 1H), 8.11 (d, 1H), 7.52 (dd, 1H), 7.35 (dd, 1H), 6.57 (s, 1H), 4.13 (q, 2H), 4.06 (s, 3H), 4.00 (2s, 5H), 1.16 (t, 3H). Anal. Calcd (found) for $C_{17}H_{18}O_5$: C, 67.54 (67.45); H, 6.00 (5.91).

Preparation of 3-Hydroxy-7,9-dimethoxyphenalenone (23). A mixture of ethyl-2,4-dimethoxy-1-naphthoylacetate (14.5 g, 0.048 mol) and polyphosphoric acid (20 mL) was stirred for 3 h at 103 °C. The reaction mixture was neutralized with 10% sodium hydroxide solution. The solution was filtered and the filtrate extracted with chloroform in several fractions. The extracts were combined and dried over anhydrous sodium sulfate, and the solvent was evaporated on a rotary evaporator to provide a concentrated solution. Addition of excess hexanes precipitated the title compound as the major product (4 g, 40%). The crude material contains some demethylated product (see the Supporting Information) that could not be separated either by column chromatography or recrystallization. The crude material was used for the next step without further purification. Mp 214−218 °C. MS (ESI), $m/z = 257$ (MH^+), 242(demethylated product). ^{1}H NMR ($CDCl_3$): δ 8.71 (d, 1H), 8.48 (d, 1H), 7.63 (t, 1H), 6.61 (s, 1H), 6.13 (s, 1H), 4.24 (s, 3H), 4.14 (s, 3H). Anal. Calcd (found) for $C_{15}H_{12}O_4$: C, 70.31 (68.87); H, 4.72 (4.36).

Preparation of 3,7,9-Trihydroxyphenalenone (24). A mixture of 3-hydroxy-7,9-dimethoxyphenalenone (1 g, 0.004 mol) and pyridine hydrochloride (3 g, 0.026 mol) was heated to 225 °C in an argon atmosphere for 15 min. The reaction was allowed to cool to room temperature and then dissolved in 200 mL 2N sodium hydroxide solution. Hydrochloric acid (3N) was added slowly to adjust the pH of the solution to 7, at which point the desired compound precipitated. The brown solid was isolated by filtration, washed several times with water, and dried (800 mg, 90% yield). Mp >300 °C. MS (ESI), $m/z = 228$. ^{1}H NMR (CD_3OD): δ 8.49 (d, 2H), 7.58 (t, 1H), 6.35 (s, 2H). Anal. Calcd (found) for $C_{13}H_8O_4$: C, 68.42 (67.75); H, 3.53 (3.51).

Preparation of 3,7-Dimethoxy-9-hydroxyphenalenone (25). 3,7,9-Trihydroxy phenalenone (800 mg, 0.0035 mol) was dissolved in acetone (200 mL) and anhydrous potassium carbonate (1.2 g, 0.0087 mol) was added. The mixture was cooled in an ice bath; methyl-*p*-toluenesulfonate (1.2 mL, 0.0087mol) was slowly added and the reaction mixture was taken to reflux. The progress of the reaction was monitored by thin layer chromatography. After 6 h, the solution was filtered and the solvent was removed from the filtrate on a rotary evaporator to give a viscous pale yellow oil. The compound was purified by column chromatography (Al_2O_3, dichloromethane). Evaporation of the solvent yielded 600 mg (67%) of a yellow solid. Mp 246 °C. MS (ESI), $m/z = 256$. ^{1}H NMR ($CDCl_3$): δ 16.67 (s, 1H), 8.41 (d, 2H), 7.53 (t, 1H), 6.42 (s, 2H), 4.07 (s, 6H). Anal. Calcd (found) for $C_{15}H_{12}O_4$: C, 70.31 (69.98); H, 4.72 (4.62).

Preparation of 17^+Cl^-. 3,7-Dimethoxy-9-hydroxyphenalenone (300 mg, 1.2 mmol) in 1,2-dichloroethane (10 mL) was treated with boron trichloride (0.6 mL of 1 M solution in dichloromethane, 0.6 mmol) under argon and the mixture was stirred for 96 h. Hexanes were added to the reaction mixture to give a yellow precipitate. The compound was isolated as a yellow solid (0.31 g, 93%) by filtration and used for the next step without further purification. MS (MALDI), $m/z = 547$(cation). ^{1}H NMR (CD_3OD): δ 8.81 (d, 4H), 7.99 (t, 2H), 7.08 (s, 4H), 4.24 (s, 12H).

Preparation of $17^+BPh_4^-$. A solution of $NaBPh_4$ (0.35 g, 1 mmol) in methanol was added to a solution of 17^+Cl^- (0.40 g, 0.72 mmol) in methanol (100 mL) and stirred for 1 h to give a yellow precipitate that was separated by filtration. The crude product was purified by recrystallization from dichloromethane/methanol to give red crystals of the desired compound (0.39 g, 64%). Mp 260 °C. MS (MALDI), $m/z = 547$(cation). ^{1}H NMR ($CDCl_3$): δ 8.72 (d, 4H), 7.82 (t, 2H), 7.3−7.4 (m, 8H), 6.92(t, 8H), 6.75 (t, 4H), 6.53 (s, 4H), 4.05 (s, 12H). Anal. Calcd (found) for $C_{54}H_{42}O_8B_2$: C, 77.16 (76.91); H, 5.04 (4.74).

Crystallization of 17. An invertible H-cell with a glass D frit was loaded in a drybox. A solution of 8 mg of $17^+BPh_4^-$ (0.009 mmol) in 12 mL of dry acetonitrile was placed in one container, and 30 mg of Cp_2Co (0.16 mmol) dissolved in 15 mL of dry acetonitrile in the other container. The H-cell was removed from the drybox and attached to the vacuum line, and the containers were taken through three cycles of freeze, pump, and thaw to degas the solutions. The H-cell was inverted slowly and the solutions were allowed to diffuse through the glass frit. After sitting in the dark for 6 h, the cell yielded 2 mg (Yield 40%) of dark red shining crystals. Anal. Calcd (found) for $C_{30}H_{22}O_8B$: C, 69.12 (68.36); H, 4.25 (4.03).

Preparation of 4-Methoxy-9-hydroxyphenalenone. 2,7-Dimethoxynaphthalene (19.0 g, 0.1 mol) and cinnamoyl chloride (16.6 g, 0.1 mol) were dissolved in 1000 mL of dry 1,2-dichloroethane. The reaction vessel was cooled in an ice bath and 13.7 g of aluminum trichloride was slowly added while the solution was mechanically stirred. After 30 min (at which time the reaction mixture had come to the room temperature), a further 13.7 g of aluminum trichloride was added and the reaction was taken to reflux. After 1 h of reflux, another 27.4 g of aluminum trichloride was added and the reaction was refluxed for 10 h. At the end of the reaction, a solid started to form that was mechanically broken up during the course of the reaction. The reaction was quenched after about 2 h by pouring into a 1:1 ice:hydrochloric acid mixture. The aqueous mixture was repeatedly extracted with methylene chloride. The organic extracts were dried over Na_2SO_4 and taken down on a rotary evaporator to give a yellow solid. The compound can be purified by sublimation and/or recrystallization from methanol, or acetonitrile to give yellow crystals (19.0 g, 84%). Mp 194 °C. ^{1}H NMR ($CDCl_3$): δ 16.44 (br, 1H), 8.53 (d, 1H), 7.97 (d, 1H), 7.94 (d, 1H), 7.16 (d, 1H), 7.04 (d, 1H), 6.98 (d, 1H), 4.11 (s, 3H). Anal. Calcd (found) for $C_{14}H_{10}O_3$: C, 74.33 (74.50); H, 4.46 (4.36).

Preparation of 18^+Cl^-. 4-Methoxy-9-hydroxyphenalenone (0.45 g, 2 mmol) and 1 mL (1 mmol) of boron trichloride (1 M solution in dichloromethane) were stirred in 50 mL of dry toluene. The reaction was refluxed for 11 h. The yellow precipitate which formed was collected by filtration and washed with toluene and dried under vacuum (0.49 g, 98%). Mp 350 °C (decomposition). The as-prepared material was used in the next reaction step without further purification.

Preparation of 18^+ $TFPB^-$. A quantity of 0.34 g (0.38 mmol) of solid sodium tetrakis[3,5-bis(trifluoromethyl)phenyl]borate (NaTFPB) was added to a solution of 18^+ Cl^- (0.2 g, 0.40 mmol) in 20 mL of dichloromethane. The mixture was stirred at 25 °C for 30 min, during which time a white precipitate formed. The reaction mixture was filtered and the filtrate was evaporated to dryness under reduced pressure. The crude material was purified by recrystallization from dichloromethane/hexane mixture, yielding 0.37 g (74%) of the analytically pure title compound. Mp 70 °C. MS (MALDI) $m/z = 461$ (cation). ^{1}H NMR ($CDCl_3$): δ, 9.05 (d, 2H), 8.47 (d, 2H), 8.38 (d, 2H), 7.72 (br, 8H), 7.49 (s, 4H), 7.39 (d, 2H), 7.32 (d, 2H), 7.28 (d, 2H), 4.25 (s, 6H). Anal. Calcd (found) for $C_{60}H_{30}B_2O_6F_{24}$: C, 54.41 (54.41), H, 2.28 (2.10).

Preparation of 19^+ Cl^-. 3,4-Dimethoxy-9-hydroxyphenalenone (0.171 g, 0.67 mmol) was dissolved in 20 mL of dry toluene by heating at 60 °C; 0.33 mL(0.33 mmol) of boron trichloride (1 M solution in dichloromethane) was added and the reaction was refluxed for 9 h. The reaction was cooled to room temperature and the yellow precipitate was collected by filtration and washed with toluene and dried under vacuum (0.15 g, 82%). Mp 234 °C (decomposition). The as-prepared material was used in the next reaction step reaction without further purification.

Preparation of 19^+ $TFPB^-$. A quantity of 0.15 g (0.17 mmol) of solid sodium tetrakis[3,5-bis(trifluoromethyl)phenyl]borate (NaTFPB) was added to a solution of 19^+ Cl^- (0.10 g, 0.18 mmol) in 20 mL of dichloromethane. The reaction was stirred at room temperature for 20 min. The reaction mixture was filtered and the filtrate was evaporated to dryness under reduced pressure. The crude material was purified by recrystallization from dichloromethane/hexane mixture, yielding 0.16 g (68%) of the analytically pure title compound. Mp 98 °C. MS (MALDI) $m/z = 521$ (cation) ^{1}H NMR ($CDCl_3$): δ, 8.35 (d, 2H), 8.33 (d, 2H), 7.71 (br, 8H), 7.49 (br, 4H), 7.38 (d, 2H), 7.26 (d, 2H), 6.76 (s, 2H), 4.22 (s, 6H), 4.18 (s, 6H). Anal. Calcd (found) for $C_{64}H_{34}B_2O_8F_{24}$: C, 55.52 (55.81), H, 2.47 (2.46).

Cyclic Voltammetry. Cyclic voltammetric measurement were performed using a CH Instruments Electrochemical Analyzer, with scan rates of 100 mV/s on solutions ($<1 \times 10^{-3}$ M) of $17^+BPh_4^-$ in oxygen-free acetonitrile (distilled from CaH_2) containing 0.1 M tetra-*n*-butylammonium hexafluorophosphate. Potentials were scanned with respect to the saturated calomel reference electrode in a single-compartment cell fitted with Pt electrodes and reference to the Fc/Fc^+ couple of ferrocene at 0.38 V vs SCE.

EPR Spectra. The EPR spectra were recorded at ambient temperature using a Bruker EMX spectrometer on crystalline samples of **17** (see the Supporting Information).

X-ray Crystallography. A black thin needle fragment ($0.43 \times 0.14 \times 0.01$ mm^3) was used for the single-crystal X-ray diffraction study of radical **17**. The crystal was mounted on to a glass fiber without coating with paratone oil. X-ray intensity data were collected at 100 and 293 K on a Bruker APEX2 (version 2.0−22) platform-CCD X-ray diffractometer system (Mo-radiation, $\lambda =$ 0.71073 Å, 50 KV/40 mA power). The CCD detector was placed at a distance of 5.0550 cm from the crystal. The crystallographic parameters and the unit-cell dimensions are summarized in Table 2. Full details, including bond lengths and difference in bond lengths between radical and cation at 100 and 293 K are given in the Supporting Information.

Magnetic Susceptibility Measurements. Magnetic susceptibility measurements on **17** were performed over the temperature range 5−305 K on a George Associates Faraday balance operating at 0.5 T. The system was calibrated using Al and Pt NIST standards.

Conductivity Measurements. The single-crystal conductivity (σ) of **17** was measured in a four-probe configuration using in-line contacts, which were attached with silver paint. The needlelike crystal was freely positioned on a sapphire substrate, and the electrical connections between the silver paint contacts on the crystal and the indium pads on the substrate were made by thin, flexible 25 μm diameter silver wires to relieve mechanical stress during thermal cycling of the crystal. The temperature dependence of the conductivity was measured in the range 300−10 K using a custom-made helium variable-temperature probe with a Lake Shore 340 temperature controller driven by LabVIEW software. A Keithley 236 unit was used as a voltage source and current meter, and two 6517A Keithley electrometers were used to measure the voltage drop between the potential leads in a four-probe configuration.

Acknowledgment. This work was supported by the Office of Basic Energy Sciences, Department of Energy, under Grant DE-FG02-04ER46138.

Appendix

In response to a referee comment, we amplify our comment that the magnetic interactions are not (solely) limited by the orbital overlap (unlike the conductivity). Part of the confusion on this topic arises from the distinction between the overlap integral between orbitals and the overlap of charge distributions. As we show below, these terms can have entirely distinct meanings.

The Heisenberg exchange term is usually obtained from the exchange integral (K) between the orbitals containing the unpaired spins and for simplicity we consider a pair of well-separated hydrogen atoms A and B [with wave functions $\Psi_A = (1s_A)^1$, $\Psi_B = (1s_B)^1$] and the first excited state of the helium atom [$\Psi(1s,2s) = (1s)^1(2s)^1$]. For a pair of well-separated hydrogen atoms, the overlap integral ($\int \Psi_A \Psi_B \, d\tau$) is small and the $1s^1$ electron densities of each atom occupy distinct regions of space, so the coulomb ($J_{A,B}$) and exchange ($K_{A,B}$) integrals involving these orbitals are also very small.

In the case of the first excited state of helium with a $1s^1$, $2s^1$ configuration [$\Psi(1s,2s) = (1s)^1(2s)^1$], it is possible to solve for the coulomb $J_{1s,2s}$ and exchange $K_{1s,2s}$ integrals between these two orbitals on the basis of the experimental energies of the excited singlet and triplet states.[57] If we assume hydrogenic 1s and 2s atomic orbitals, they must be rigorously orthogonal and the orbital overlap is zero ($\int 1s\ 2s \, d\tau = 0$), yet the exchange integral amounts to $K_{1s,2s} = 3200$ cm^{-1}. Another way to say this is that the proximity and the phase of the interacting orbitals are both important in determining the overlap integral, but the coulomb and exchange integrals are (mainly) dependent on the proximity of the electron densities of the spin−orbitals. Thus in our case (above), even though the bandwidth is driven close to zero at room temperature by the low overlap integral between the spin containing molecular orbitals of the molecules (which determines the off-diagonal elements of the EHT Hamiltonian), a value of 36 cm^{-1} is not unreasonable for the exchange interaction.

Supporting Information Available: Crystallographic CIF files of **17**, $17^+BPh_4^-$, 18^+TFPB^-, 19^+TFPB^-; regression analysis data, ^{1}H NMR and mass spectra of compound **23** and 17^+Cl^-, ESR spectra of radical **17**, full literature citation for ref 3 (PDF). This material is available free of charge via the Internet at http://pubs.acs.org.

CM900242A

(57) Kauzmann, W. *Quantum Chemistry*; Academic Press: New York, 1957.